Special issue of the 3rd International Conference on Computational and Experimental Science and Engineering (ICCESEN 2016)

Experimental and Quantum Chemical Calculations of 2-Amino-4,5,6,7-Tetrahydrobenzo[b]Thiophene-3-Carbonitrile

H. Oturak[a,*], N. Kaya Kinaytürk[b], M.A. Topuz[a], N. Kutlu[a], E. Kaynaker[a], P. Talip[a] and Y. Sert[c]

[a]Süleyman Demirel University, Physics Department, Isparta, Turkey

[b]Süleyman Demirel University, Experimental and Observational Research and Application Centre, Isparta, Turkey

[c]Department of Physics, Faculty of Art and Sciences, Bozok University, Yozgat 66100, Turkey

Vibrational frequencies of 2-Amino-4,5,6,7-Tetrahydrobenzo[b]Thiophene-3-Carbonitrile were calculated using density functional (DFT/B3YLP) method with 6-311++G(d,p) basis set by Gaussian 09. The assignments of the vibrational frequencies have been done by potential energy distribution analysis, using VEDA 4 software. The density functional theory and time dependent density functional theory methods have been used to study the electronic properties of 2-Amino-4,5,6,7-Tetrahydrobenzo[b]Thiophene-3-Carbonitrile. Isotropic chemical shifts were calculated using the gauge-invariant atomic orbital method. All computed spectroscopic properties were compared with experimental ones. The simulated spectra of the molecule show excellent agreement with the experimental spectra.

DOI: 10.12693/APhysPolA.132.1192

PACS/topics: 31.15.E–, 33.20.Ea, 33.20.Tp, 33.20.Fb, 33.20.Lg, 33.20.Bx

1. Introduction

Thiophene is one of the simplest aromatic molecules with a five membered heterocyclic sulphur-containing ring. Thiophene obeyes the $4n + 2\pi$ electron rule and is considered to be aromatic. Thiophene is uniquely an electron rich heterocycle and has the highest resonance stabilization energy among the five membered heterocycles. Thiophenes are part of many organic compounds having vast applications in the field of electronics and optoelectronics, medicine and materials.

The compounds, containing a thiophene ring in their structure have a remarkable pharmacological efficiency. They are known for their antidepressant, anticonvulsant, anthelmintic, antispasmodic, antihistaminic, anesthetic, antipruritic, antitussive and analgesic action. Thiophene and its derivatives exhibit diverse biological properties, such as nemoticial, insecticidal, antibacterial, antifungal, antiviral and antioxidant activity [1–15].

The molecular structure of the title compound, 2-Amino-4,5,6,7-Tetrahydrobenzo[b]Thiophene-3-Carbonitrile (ATHBTCN), has been studied by single crystal X-ray spectroscopy [1]. Although X-ray diffraction method is one of the most frequently applied techniques for structural characterization of pharmaceutical compounds, the use of vibrational spectroscopy is also gaining increasing attention. X-ray diffraction techniques are sensible to the long range order while vibrational spectroscopy (IR and Raman) is applicable to the short-range structure of molecular solids. As the literature survey reveals, neither IR and Raman spectra nor quantum chemical calculations of the compound have been reported so far. Hence the present work was undertaken to study the vibrational spectra by quantum chemical calculations. We have interpreted the calculated spectra in terms of potential energy distribution (PED).

2. Experimental and computation details

The compounds of ATHBTCN in solid form were purchased from Sigma-Aldrich chemical company (U.S.A.) with a purity of greater than 98%, and were used as such, without further purification. The FT-IR spectrum was recorded using KBr pellets on a Perkin Elmer Spectrum BX FTIR spectrophotometer in the region of 4000–400 cm^{-1}. The FT-Raman spectrum was obtained on a DXR-Raman Microscope in the region of 3500–12 cm^{-1}. The ^{1}H and ^{13}C NMR were taken in DMSO solutions on a Bruker Ultrashield 400 Plus NMR spectrometer. Proton and carbon signals were referenced to TMS. UV-visible spectroscopy analyses were carried out using a Perkin Elmer Lambda 20 spectrofotometer. All spectra were measured at room temperature.

Gaussian 09 [16] software package was used for the theoretical calculations. The quantum chemical calculations were performed by applying the density functional theory (DFT) method, with the B3LYP functional and the 6-311G++(d,p) basis set. Since B3LYP vibrational wavenumbers are known to be higher than the experimental wavenumbers due to neglect of anharmonicity effects, they were scaled down by a uniform scaling factor of 0.983 for wavenumbers up to 1700 cm^{-1} and 0.958 for wavenumbers greater than 1700 cm^{-1} [17]. The scaled wavenumbers in general show good agreement with experimental ones.

*corresponding author; e-mail: haliloturak@sdu.edu.tr

The geometry optimizations were followed by frequency calculations using the same basis set. The same basis set and functional were also used for the calculations of ^{1}H and ^{13}C NMR shielding constants, by applying the GIAO method. UV-Vis spectra and electronic properties were determined by time-dependent DFT (TD-DFT). The results were visualized using Gauss View program [18]. Initial atomic coordinates can be generally taken from any database or experimental XRD results. We have used the experimental XRD data and Gauss View software database to determine the initial atomic coordinates and to optimize the input structure. After the optimization, we have used the most stable optimized structure for further theoretical analysis.

In this study, initial atomic coordinates that were taken from Gauss View database [18] have given most stable structure after optimization. Total energy distribution corresponding to the observed frequencies was calculated using VEDA 4 program [19].

3. Results and discussion

3.1. Geometric structure

The single X-ray crystallographic analysis of the title compound ($C_9H_{10}N_2S$) shows that its crystal belongs to space group $P2_1/c$ and belongs to monoclinic system with the following cell dimensions: $a = 10.4274$ Å, $b = 8.1487$ Å, $c = 13.2342$ Å, $\beta = 126.937°$ and $V = 898.81$ Å^3 [1]. The theoretical and experimental structure parameters (bond lengths, bond angles and torsion angles) are shown in Table I, in accordance with the atom-numbering scheme, given in Fig. 1.

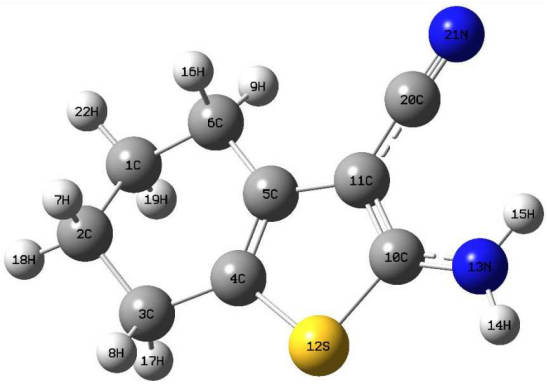

Fig. 1. Optimized structure of ATHBTCN.

When we look at the key data for our compound: in carbonitrile group, C11–C20 and C20≡N21 bond lengths have been recorded as 1.417 Å and 1.145 Å, respectively. These bond lengths have been calculated as 1.4132 Å and 1.1598 Å, respectively by B3LYP method. In thiophene ring C4–S12 and C10–S12 bond lengths have been reported as 1.7432 Å and 1.7280 Å, respectively. These data have been calculated as 1.7691 Å and 1.7462 Å, respectively. Finally, C5=C4 bond length has been observed as 1.346 Å. We have calculated this length as 1.366 Å with B3LYP method.

TABLE I

Optimized parameters of ATHBTCN.

Parameters	X-ray [1]	B3LYP 6311++G(d,p)
Bond lengths		
S12–C10	1.728	1.7462
S12–C4	1.743	1.7691
N21–C20	1.145	1.1598
N13–C10	1.351	1.3612
N13–H14	0.860	1.0039
N13–H15	0.860	1.0073
C11–C10	1.383	1.3855
C11–C20	1.417	1.4132
C11–C5	1.438	1.4480
C5–C4	1.346	1.3665
C5–C6	1.502	1.5066
C6–C1	1.530	1.5375
C6–H9	0.9700	1.0947
C6–H16	0.9700	1.0978
C1–C2	1.509	1.5351
C1–H19	0.970	1.0965
C1–H22	0.970	1.0937
C2–C3	1.526	1.5351
C2–H7	0.970	1.0961
C2–H18	0.970	1.0938
C3–C4	1.502	1.5014
C3–H8	0.970	1.0953
C3–H17	0.9700	1.0981
Bond angles [°]		
C10–S12–C4	92.09	91.6901
C10–N13–H14	120.0	121.8968
C10–N13–H15	120.0	119.7581
H14–N13–H15	120.0	118.3448
C10–C11–C20	121.99	121.3968
C10–C11–C5	113.48	113.0574
C20–C11–C5	124.47	125.5452
C4–C5–C11	112.23	113.0603
C4–C5–C6	122.47	122.1610
C11–C5–C6	125.29	124.7771
C5–C6–C1	110.43	111.2581
C5–C6–H9	109.6	109.9205
C1–C6–H9	109.6	110.3649
C5–C6–H16	109.6	109.2059
C1–C6–H16	109.6	110.0731
H9–C6–H16	108.1	105.8717
C2–C1–C6	111.65	111.6692
C2–C1–H19	109.3	109.1527
C6–C1–H19	109.3	109.2828
C2–C1–H22	109.3	110.2162
C6–C1–H22	109.3	109.6786
H19–C4–H22	108.0	106.7088
C1–C2–C3	111.88	111.5164
C1–C2–H7	109.2	109.2407
C3–C2–H7	109.2	109.1132
C1–C2–H18	109.2	110.4469
C3–C2–H19	109.2	109.4775

TABLE I cont.

Optimized parameters of ATHBTCN.

Parameters	X-ray [1]	B3LYP 6311++G(d,p)
Bond angles [°]		
H7–C2–H19	107.9	106.9275
C4–C3–C2	109.33	109.5923
C4–C3–H8	109.8	110.8944
C2–C3–H8	109.8	109.9175
C4–C3–H17	109.8	110.2467
C2–C3–H17	109.8	109.8390
H8–C3–H17	108.3	106.3030
C5–C4–C3	125.82	126.2009
C5–C4–S12	111.97	111.3386
C3–C4–S12	122.20	122.4987
N13–C10–C11	128.53	127.5120
N13–C10–S12	121.26	121.6358
C11–C10–S12	110.21	110.8521
N21–C20–C11	178.84	177.7332

Similarly, when we look at the key bond angle data: C4–S12–C10, S12–C10–N13 and C5–C11–C20 have been reported as 92.09°, 121.26° and 124.47°, respectively. We have calculated these angles as 91.6901°, 121.6358° and 125.5452°, respectively.

3.2. Vibrational analysis

The experimental FT-IR and FT-Raman spectra of the title compound are compared with the theoretical spectra in Figs. 2 and 3, respectively. The scaled calculated harmonic vibrational frequencies at B3LYP level, observed vibrational frequencies, and detailed PED assignments are tabulated in Table II. Harmonic frequencies are calculated for gas phase of an isolated compound, although the experimental ones are obtained for its solid phase. Therefore, there is a disagreement between the observed and calculated frequencies in some modes.

TABLE II

Detailed assignments of experimental and theoretical wavenumbers of ATHBTCN, along with potential energy distribution.

DFT-B3LYP-6311++G(d,p)		Experimental		Assignment
non-scaled	scaled	IR	Raman	
3737	3561	3445	3444	$\nu_{NH}(97)$
3609	3439	3327	3326	$\nu_{NH}(97)$
3068	2924	2956		$\nu_{CH}(93)$
3065	2921	2930	2936	$\nu_{CH}(98)$
3051	2908	2909	2912	$\nu_{CH}(92)$
3040	2897		2889	$\nu_{CH}(87)$
3021	2879			$\nu_{CH}(85)$
3014	2872		2868	$\nu_{CH}(88)$
3004	2863	2853		$\nu_{CH}(91)$
2995	2854	2836	2838	$\nu_{CH}(98)$
2297	2189	2197	2196	$\nu_{NC}(88) + \nu_{CC}(12)$
1650	1581	1616	1618	$\delta_{HNH}(86)$
1626	1558	1590	1589	$\nu_{CC}(83)$
1546	1481	1521	1518	$\nu_{CC}(53) + \nu_{NC}(24)$
1502	1439	1444	1446	$\delta_{HCH}(88)$
1492	1429	1433		$\delta_{HCH}(87)$
1489	1426		1429	$\delta_{HCH}(84)$
1479	1417	1399		$\delta_{HCH}(81)$
1423	1363		1399	$\nu_{CC}(31) + \tau_{HCCC}(10)$
1382	1324	1339	1333	$\delta_{HCC}(10) + \tau_{HCCC}(60)$
1371	1313	1330		$\tau_{HCCC}(61)$
1367	1310			$\delta_{HCC}(37) + \tau_{HCCC}(22)$
1360	1303	1282		$\nu_{CC}(11) + \tau_{HCCC}(20)$
1311	1256	1251	1255	$\nu_{NC}(16) + \nu_{CC}(12) + \delta_{HCC}(27)$
1282	1228	1235		$\delta_{HCC}(22) + \tau_{HCCC}(25)$
1269	1216		1197	$\delta_{HCC}(48) + \tau_{HCCC}(11) + \tau_{CCCC}(13)$
1204	1153	1164	1168	$n_{CC}(11) + \delta_{HNC}(12) + \tau_{HCCC}(12)$
1187	1137	1127		$\delta_{HNC}(18) + \tau_{HCCC}(31)$
1163	1114		1129	$\delta_{HCC}(66)$

TABLE II cont.

Detailed assignments of experimental and theoretical wavenumbers of ATHBTCN, along with potential energy distribution.

DFT-B3LYP-6311++G(d,p)		Experimental		Assignment
non-scaled	scaled	IR	Raman	
1132	1084	1063		$\nu_{CC}(21) + \delta_{HNC}(27)$
1101	1055			$\delta_{HCC}(24) + \tau_{CCCC}(35)$
1079	1034	1023		$\nu_{CC}(51) + \delta_{CCC}(12) + \tau_{HCCC}(11)$
1025	982	971		$\delta_{CCC}(16) + \tau_{HCCC}(13)$
982	941	949		$\nu_{CC}(50)$
959	919			$\nu_{CC}(19) + \delta_{CCC}(28)$
918	879	852	851	$\tau_{HCCC}(46) + \tau_{CCCC}(16)$
853	817	818	821	$\nu_{CC}(43)$
834	799			$\delta_{HCC}(15) + \tau_{HCCC}(51) + \tau_{CCCC}(12)$
826	791	765		$\nu_{SC}(20) + \delta_{HNC}(10) + \delta_{CCC}(12)$
769	737			$\nu_{SC}(12) + \delta_{SCC}(12) + \delta_{CCC}(10) + \tau_{HCCC}(12)$
672	644	657		$\tau_{NCCC}(14) + \gamma_{CCCC}(36) + \gamma_{NCSC}(18)$
614	588		606	$\nu_{CC}(25) + \delta_{CCC}(11)$
560	536	547	556	$\nu_{SC}(17) + \delta_{NCC}(16) + \delta_{CCC}(12) + \gamma_{CCCC}(12)$
551	528		495	$\tau_{HCCC}(14)$
544	521	497	468	$\delta_{CCC}(12) + \tau_{HCCC}(14) + \gamma_{CCCC}(15)$
497	476	472	453	$\tau_{NCCC}(61) + \gamma_{NCSC}(22)$
470	450	450	403	$\nu_{CC}(15) + \nu_{SC}(16) + \delta_{SCC}(39)$
454	435		382	$\nu_{CC}(15) + \delta_{CCC}(38)$
404	387			$\delta_{NCC}(18) + \delta_{CCC}(18) + \delta_{NCS}(25)$
382	366		306	$\delta_{CCC}(28) + \delta_{NCS}(22)$
345	331			$\tau_{HNCC}(94)$
326	312			$\tau_{HNCC}(63) + \tau_{CCCC}(10)$
296	284			$\delta_{CCC}(18) + \tau_{HNCC}(18) + \tau_{HCCC}(19) + \tau_{CCCC}(10)$
293	281			$\tau_{HCCC}(11) + \tau_{CCCC}(22) + \tau_{SCCC}(12) + \gamma_{NCSC}(17)$
241	231		223	$\delta_{CCC}(34) + \delta_{NCS}(32)$
213	204			$\tau_{HCCC}(11) + \tau_{CCCC}(20) + \gamma_{CCCC}(20) + \gamma_{NCSC}(11)$
160	153		157	$\tau_{CCCC}(18) + \tau_{SCCC}(49)$
113	108			$\delta_{NCC}(37) + \delta_{CCC}(54)$
96	92			$\tau_{CCCC}(24) + \gamma_{CCCC}(42)$
89	85			$\tau_{CCCC}(41) + \gamma_{CCCC}(20)$

In order to introduce the detailed vibrational assignments of the compound, the PED analysis has been carried out and results are given in Table II. All calculated modes are numbered from the largest to the smallest frequency, within each fundamental wave number, in the Table II.

3.2.1. Thiophene vibrations

The C–S bands cannot be distinguished in thiophenes. This fact can be explained due to the shorter bond length and higher polarity of the C–S bond in thiophenes [20]. Klots et al. [21] assigned this mode at 872 cm^{-1}, 753 cm^{-1} and 870 cm^{-1}; 750 cm^{-1} to vapor and liquid phases, respectively. The C–S stretching mode is predicted at 691 cm^{-1}, 707 cm^{-1} and recorded at 743 cm^{-1} and 771 cm^{-1} [22].

In this work, the C–S stretching modes were observed in FT-IR and FT-Raman spectra at 765 cm^{-1} (IR), 547/556 cm^{-1} (FT-IR/FT-Raman) and 450/403 cm^{-1} (FT-IR/FT-Raman). These modes (scaled) have been calculated to be at 791 cm^{-1}, 737 cm^{-1}, 536 cm^{-1} and 450 cm^{-1} by DFT/B3LYP method with 6-311++G(d,p) basis set.

In plane bending modes: δ_{SCC} was calculated at 737 cm^{-1} by scaled B3LYP, but this mode was not observed neither in FT-IR, nor in FT-Raman spectra. Also, δ_{SCC} bending modes were seen at 306 cm^{-1} and 223 cm^{-1} in FT-Raman spectrum. These modes were calculated to be at 387 cm^{-1}, 366 cm^{-1} and 231 cm^{-1} by scaled B3LYP method.

Out-of-plane modes: γ_{NCSC} were observed at 657 cm^{-1} (FT-IR), 472 cm^{-1}/453 cm^{-1} (FT-IR/FT-Raman), respectively. These modes were calculated to be at 644 cm^{-1}, 476 cm^{-1}, 281 cm^{-1} and 204 cm^{-1} by scaled B3LYP. Other out-of-plane modes are τ_{SCCC}. These modes were observed at 157 cm^{-1} in FT-Raman

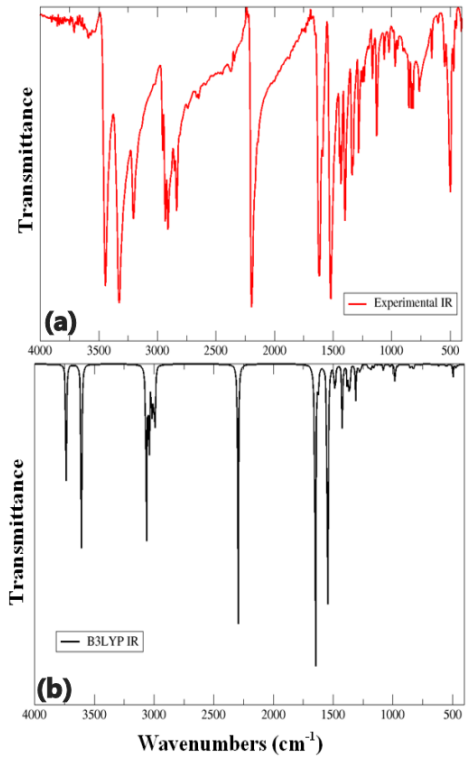

Fig. 2. Comparison of observed and calculated infrared spectra of the title compound.

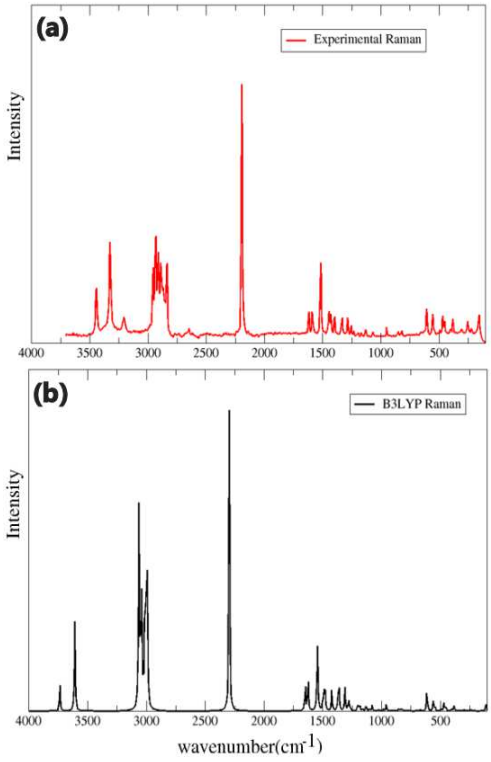

Fig. 3. Comparison of observed and calculated Raman spectra of the title compound.

spectrum. These modes were not observed in FT-IR, and were calculated to be at 281 cm^{-1} and 153 cm^{-1} by scaled B3LYP method.

3.2.2. Amino group vibrations

In primary amines, usually the N–H stretching vibrations occur in the region of 3500–3300 cm^{-1} [23–25]. The NH_2 group has two vibrations; one is being asymmetric and other symmetric. The frequency of asymmetric vibration is higher than that of symmetric one. In the present study, the asymmetric and symmetric NH stretching vibrations were identified at 3445/3444 cm^{-1} (FT-IR/FT-Raman) and 3327/3326 cm^{-1} (FT-IR/FT-Raman), respectively. The same bands were calculated to be at 3561 and 3439 cm^{-1} by scaled B3LYP/6-311++G(d,p) method. As expected, these two modes are pure stretching modes, as it is evident from PED column, they are contributing almost 100%. It is also observed that, the asymmetric band is more intense than the symmetric one. These assignments are in line with the literature [26, 27].

The N–H in-plane bending vibrations (scissoring) are usually observed in the region of 1610–1630 cm^{-1}, rocking vibrations are assigned in the range of 1100–1200 cm^{-1} and the out of plane bending (wagging and twisting) vibrations are normally identified under 900 cm^{-1} [28–31]. In this case, in plane bending mode δ_{HNH} was observed at 1616/1618 cm^{-1} (FT-IR/FT-Raman) and was calculated to be at 1581 cm^{-1} by scaled B3LYP.

Similarly, in-plane rocking modes were observed at 1164/1168 cm^{-1} (FT-IR/FT-Raman), 1127 cm^{-1} (FT-IR) and 1063 cm^{-1} (FT-IR), and these modes were calculated to be at 1153 cm^{-1}, 1137 cm^{-1} and 1084 cm^{-1} by scaled B3LYP method.

The N–H out-of-plane bending modes were assigned to and observed at 657 cm^{-1} (FT-IR), 472/453 cm^{-1} (FT-IR/FT-Raman). These modes were calculated to be at 644 cm^{-1}, 476 cm^{-1}, 281 cm^{-1} and 204 cm^{-1} by B3LYP method. According to the literature, these assignments agree well. The N–H vibrations have not been affected by the vibrations of other substituents.

3.2.3. Carbonitrile group vibrations

Unsaturated or aromatic nitriles, in which the double bond or ring is adjacent to C≡N group, absorb more strongly in infrared region than saturated compounds, and the related band occurs at somewhat lower frequency, near 2230 cm^{-1} [32]. In the present study, the computed value is assigned to the stretching of C≡N group, and it is in a good agreement with our experimental spectrum; the observed band in FT-IR spectrum at 2197 cm^{-1} and 2196 cm^{-1} in FT-Raman spectrum. The vibrational mode calculated to be at 2189 cm^{-1} by scaled B3LYP methods is assigned to the in-plane stretching vibration of C≡N group. In addition, in the carbonitrile group (C11–C20) $\nu_{C\text{-}C}$ mode has been observed at 2197 cm^{-1} in FT-IR and at 2196 cm^{-1} in FT-Raman spectra. This mode has been calculated to be at 2189 cm^{-1} by scaled B3LYP method.

3.2.4. Tetrahydrobenzo group vibrations

The CH_2 group has 24 vibrational modes (4 asymmetrical and 4 symmetrical stretching modes, 4 scissoring modes, 4 wagging modes, 4 twisting modes and 4 rocking modes). The asymmetric stretching CH_2, symmetric stretching CH_2, scissoring vibrations CH_2, and the wagging vibration CH_2 appear in the regions of 3000 ± 20, 2900 ± 25, 1440 ± 10 and 1340 ± 25 cm^{-1}, respectively [33, 34].

For our compound the CH_2 asymmetric stretching modes are observed at 2956 cm^{-1} (FT-IR), 2930/2936 cm^{-1} (FT-IR/FT-Raman), 2909/2912 cm^{-1} (FT-IR/FT-Raman) and 2889 cm^{-1} (FT-Raman). These asymmetric stretching modes have been calculated to be at 2924 cm^{-1}, 2921 cm^{-1}, 2908 cm^{-1} and 2897 cm^{-1} by the scaled B3LYP method.

Similarly, for our compound the CH_2 symmetric stretching modes are observed at 2853 cm^{-1} (FT-IR) and 2836/2838 cm^{-1} (FT-IR/FT-Raman). These symmetric stretching modes have been calculated to be at 2879 cm^{-1}, 2872 cm^{-1}, 2863 cm^{-1} and 2854 cm^{-1} by the scaled B3LYP method.

The CH_2 scissoring modes have been observed at 1444/1446 cm^{-1} (FT-IR/FT-Raman), 1433 cm^{-1} (FT-IR), 1429 cm^{-1} (FT-Raman) and 1399 cm^{-1} (FT-IR). These scissoring modes have been calculated to be at 1439 cm^{-1}, 1429 cm^{-1}, 1426 cm^{-1} and 1417 cm^{-1}.

The CH_2 wagging modes have been observed at 1399 cm^{-1} (FT-Raman), 1339/1333 cm^{-1} (FT-IR/FT-Raman) and 1330 cm^{-1} (FT-IR). These wagging modes have been calculated to be at 1363 cm^{-1}, 1324 cm^{-1}, 1313 cm^{-1} and 1310 cm^{-1}.

The CH_2 twisting and rocking modes appear in the regions [33] of 1260 ± 10 and 800 ± 25 cm^{-1}. For our title compound, the CH_2 twisting modes have been observed at 1251/1255 cm^{-1} (FT-IR/FT-Raman), 1235 cm^{-1} (FT-IR), 1197 cm^{-1} (FT-Raman), 1164/1168 cm^{-1} (FT-IR/FT-Raman). These twisting modes have been calculated to be at 1256 cm^{-1}, 1228 cm^{-1}, 1216 cm^{-1} and 1153 cm^{-1} by scaled B3LYP.

Finally, the CH_2 rocking modes have been observed at 971 cm^{-1} (FT-IR) and 852/851 cm^{-1} (FT-IR/FT-Raman), these rocking modes have been calculated to be at 982 cm^{-1}, 879 cm^{-1}, 799 cm^{-1} and 737 cm^{-1} by scaled B3LYP method.

In the ring $\nu_{C4=C5}$ has been observed at 1590/1589 cm^{-1} (FT-IR/FT-Raman) and calculated to be at 1558 cm^{-1} by scaled B3LYP method. Other modes within the $\nu_{C=C}$ have been observed at 1164/1168 cm^{-1} (FT-IR/FT-Raman), 1063 cm^{-1} (FT-IR) and 1023 cm^{-1} (FT-IR). These modes have been calculated to be at 1153 cm^{-1}, 1084 cm^{-1} and 1034 cm^{-1} by scaled B3LYP method.

3.3. NMR analysis

The theoretical and experimental chemical shifts of ^{13}C and ^{1}H and the assignments of ATHBTCN is shown in Table II. The experimental ^{13}C and ^{1}H NMR spectra are presented in Fig. 4a and b. In recent years, gauge-including atomic orbital GIAO computational method is efficient in predicting chemical shifts of various organic compounds [35].

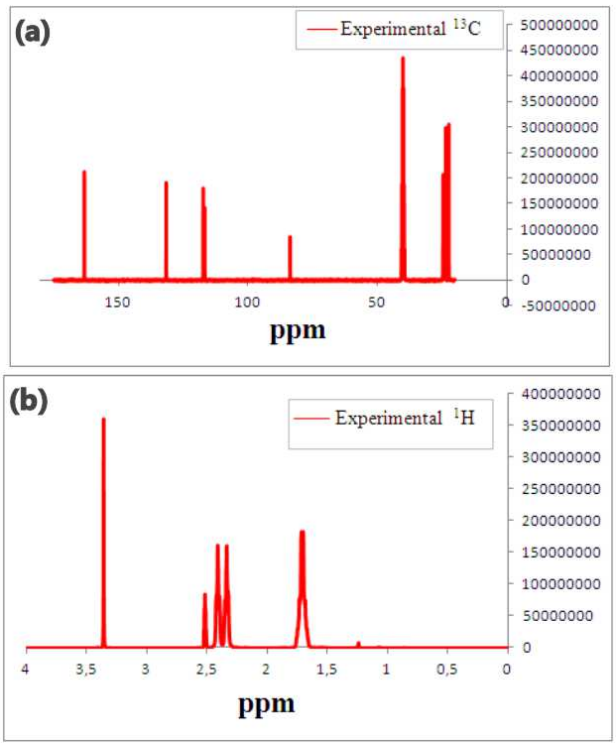

Fig. 4. The experimental ^{13}C and ^{1}H NMR spectra.

In this study, the optimized structure of ATHBTCN is used to calculate the NMR spectra by the DFT/B3LYP method with 6-311++G(d,p) level using the GIAO method. The result in Table III shows that the range of ^{13}C NMR chemical shift of the typical organic molecule usually is > 100 ppm which ensures a reliable interpretation of spectroscopic parameters [36, 37]. In this study, ^{13}C NMR chemical shifts in the ring of the title molecule are > 100 ppm, as was expected.

TABLE III

^{13}C and ^{1}H NMR shifts for ATHBTCN.

ATOM	B3LYP [ppm]	Exp. [ppm]	ATOM	B3LYP [ppm]	Exp. [ppm]
C(1)	26.36	24.49	H(7)	1.65	1.70
C(2)	28.01	39.58	H(8)	2.39	2.33
C(3)	28.39	39.98	H(9)	2.57	2.53
C(4)	129.75	117.29	H(14)	4.24	3.94
C(5)	139.91	131.58	H(15)	4.52	3.36
C(6)	29.17	40.20	H(16)	2.43	2.34
C(10)	170.72	163.23	H(17)	2.55	2.52
C(11)	88.49	83.68	H(18)	1.84	1.73
C(20)	118.95	116.67	H(19)	1.57	1.68
			H(22)	1.8	1.71

3.4. UV analysis

On the basis of fully optimized ground-state structure, the TD-DFT-B3LYP-6311++G(d,p) method was used to determine the low-lying excited states of ATHBTCN. The calculated excitation energies, oscillator strength f and wavelength λ and spectral assignments were carried out and compared with measured experimental wavelengths, given in Table IV.

According to the calculation results, three sharp electronic transitions were observed for title molecule (274, 277, 310 nm for ATHBTCN in DMSO), in good agreement with the measured experimental data, as shown in Fig. 5. According to Frank-Condon principle, the maximum absorption peaks correspond in an UV-visible spectrum to vertical excitation [36].

TABLE IV

Excitation energies for ATHBTCN.

$\lambda_{cal.}$	$\lambda_{exp.}$	E [eV]	f	Assignment	Major contribution
310		3.9969	0.0011	$n\rightarrow\pi^*$	HOMO→LUMO+1
277	290	4.4690	0.1040	$\pi\rightarrow\pi^*$	HOMO→LUMO
274		4.5181	0.0084	$n\rightarrow\pi^*$	HOMO→LUMO+2

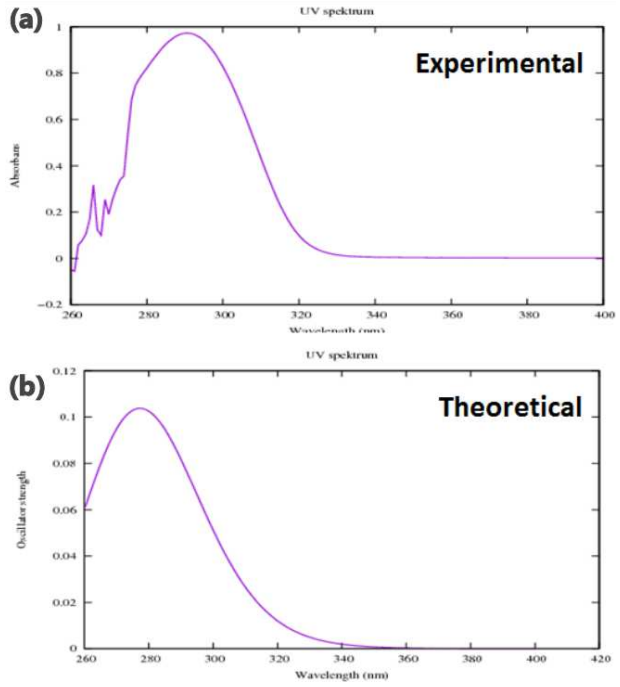

Fig. 5. Experimental and theoretical UV spectrum of ATHBTCN.

4. Conclusions

In this study, the vibrational analysis of ATHBTCN molecule was carried out using experimental FT-IR spectroscopy, and theoretical calculations (DFT/B3LYP method). The optimized geometric parameters, vibrational harmonic frequencies and PED assignments for the compound have been calculated using DFT/B3LYP method with 6-311++G(d,p) basis set. The theoretical optimized geometric parameters (bond lengths and angles) and vibrational frequencies were compared with the experimental data. Considerable level of correlation has been noticed. The detailed PED analysis of the compound has shown a good agreement with the experimental data. Besides, the ^{13}C NMR and ^{1}H NMR chemical shifts and UV spectra were obtained by the DFT/B3LYP methods, using 6-311++G(d,p) basis set, in accordance with experimental results.

Acknowledgments

Authors would like to extend their appreciation to Scientific Research at Suleyman Demirel University for funding this research through the research project 3555-YL2-13.

References

[1] W.L. Silva, M.C. Lima, S.L. Galdino, I.R. Pitta, C.A. Simone, *Acta Cryst.* **E67**, o3161 (2011).

[2] J.D. Magdaline, T. Chithambarathanu, *J. Appl. Chem.* **8**, 6 (2015).

[3] J.L. Reddinger, J.R. Reynolds, *Adv. Polym. Sci.* **145**, 57122 (1999).

[4] D.T. McQuade, A.E. Pullen, T.M. Swager, *Chem. Rev.* **100**, 2537 (2000).

[5] I.C. Choong, W. Lew, D. Lee, P. Pham, M.T. Burdett, J.W. Laam, C. Wiesmann, T.N. Luong, B. Fahr, W.L. DeLano, R.S. McDowell, D.A. Allen, D. Erlanson, E.M. Gordon, T. O'Brien, *J. Med. Chem.* **45**, 5005 (2002).

[6] K. Dore, S. Dubus, H.A. Ho, I. Levesque, M. Brunette, G. Corbeil, M. Boissinot, G. Boivin, M.G. Bergeron, D. Boudreau, M. Leclerc, *J. Am. Chem. Soc.* **126**, 4240 (2004).

[7] D.K. James, J.M. Tour, *Topics Curr. Chem.* **257**, 33 (2005).

[8] P. Si, Q. Chi, Z. Li, J. Ulstrup, P.J. Moller, J. Mortensen, *J. Am. Chem. Soc.* **129**, 3888 (2007).

[9] *Merck Index*, 13th ed., Merck & Co, Whitehouse Station, New Jersery 2001.

[10] J. Bakker, F.J. Gommers, I. Nieuwenhius, H. Wynberg, *J. Biol. Chem.* **254**, 1841 (1979).

[11] S. Iyengar, J.T. Arnason, B.J.R. Philogene, P. Morand, N.H. Werstiuk, G. Timmins, *Pesticide Biochem. Physiol.* **29**, 1 (1987).

[12] H. Matsuura, G. Saxena, S.W. Farmer, R.E.W. Hancock, G.H. Towers, *Planta Med.* **62**, 256 (1996).

[13] G.F.Q. Chan, G.H.N. Towers, J.C. Mitchell, *Phytochem.* **14**, 2295 (1975).

[14] J.B. Hudson, E.A. Graham, N. Miki, G.H.N. Towers, L.L. Hudson, R. Rossi, A. Carpita, D. Neri, *Chemosphere* **19**, 1329 (1989).

[15] J. Malmstrom, M. Jonsson, I.A. Cotgreave, L. Hammarstrom, M. Sjodin, L. Engmann, *J. Am. Chem. Soc.* **123**, 3434 (2001).

[16] M.J. Frisch, G.W. Trucks, H.B. Schlegel, G.E. Scuseria, M.A. Robb, J.R. Cheeseman, G. Scalmani, V. Barone, B. Mennucci, G.A. Petersson, H. Nakatsuji, M. Caricato, X. Li, H.P. Hratchian, A.F. Izmaylov, J. Bloino, G. Zheng, J.L. Sonnenberg, M. Hada, M. Ehara, K. Toyota, R. Fukuda, J. Hasegawa, M. Ishida, T. Nakajima, Y. Honda, O. Kitao, H. Nakai, T. Vreven, J.A. Montgomery Jr., J.E. Peralta, F. Ogliaro, M. Bearpark, J.J. Heyd, E. Brothers, K.N. Kudin, V.N. Staroverov, R. Kobayashi, J. Normand, K. Raghavachari, A. Rendell, J.C. Burant, S.S. Iyengar, J. Tomasi, M. Cossi, N. Rega, J.M. Millam, M. Klene, J.E. Knox, J.B. Cross, V. Bakken, C. Adamo, J. Jaramillo, R. Gomperts, R.E. Stratmann, O. Yazyev, A.J. Austin, R. Cammi, C. Pomelli, J.W. Ochterski, R.L. Martin, K. Morokuma, V.G. Zakrzewski, G.A. Voth, P. Salvador, J.J. Dannenberg, S. Dapprich, A.D. Daniels, Ö. Farkas, J.B. Foresman, J.V. Ortiz, J. Cioslowski, D.J. Fox, *Gaussian 09*, revision A.1. Gaussian, Inc., Wallingford CT 2009.

[17] N. Sundaraganesan, S. Ilakiamania, H. Saleema, P.M. Wojciechowski, D. Michalska, *Spectrochim. Acta Part A* **61**, 2995 (2005).

[18] R. Dennington, T. Keith, J. Millam, *Gaussview Ver. 5. s.l.*: Semichem Inc. Shawnee Mission, KS 2009.

[19] M.H. Jamróz, *Vibrational Energy Distribution Analysis*, VEDA 4 Computer Program, Warsaw 2004.

[20] C.I. Sainz-Diaz, M. Francisco-Marquez, A. Vivier-Bunge, *Theor. Chem. Acc.* **125**, 83 (2010).

[21] T.D. Klots, R.D. Chirico, W.V. Steele, *Spectrochim. Acta Part A* **50**, 765 (1994).

[22] M. Karabacak, M. Çınar, M. Kurt, *J. Mol. Struct.* **968**, 108 (2010).

[23] Y. Wang, S. Saebo, C.V. Pittman, *J. Mol. Struct. (THEOCHEM)* **281**, 91 (1993).

[24] S. Sudha, N. Sundaraganesan, M. Kurt, M. Cinar, M. Karabacak, *J. Mol. Struct.* **985**, 148 (2011).

[25] N. Puviarasan, V. Arjunan, S. Mohan, *Turkey J. Chem.* **26**, 323 (2002).

[26] M. Karabacak, M. Kurt, A. Ataç, *J. Phys. Organic Chem.* **22**, 321 (2009).

[27] A. Usha Rani, N. Sundaraganesan, M. Kurt, M. Cinar, M. Karabacak, *Spectrochim. Acta Part A* **75**, 1523 (2010).

[28] H.F. Hameka, J.O. Jensen, *J. Mol. Struct. (THEOCHEM)* **362**, 325 (1996).

[29] J.R. During, M.M. Bergana, H.V. Phan, *J. Raman Spectroscopy* **22**, 141 (1991).

[30] G. Varsanyi, *Vibrational Spectra of Benzene Derivatives*, Academic Press, New York 1969.

[31] Z. Niu, K.M. Dunn, J.E. Boggs, *J. Mol. Phys.* **55**, 421 (1985).

[32] J.B. Labbert, H.F. Shurvel, L. Verbit, R.G. Cooks, G.H. Stout, *Organic Structural Analysis*, Macmillan Publ. Co. Inc., New York 1976.

[33] N.P.G. Roeges, *A Guide to the Complete Interpretation of Infrared Spectra of Organic Structures*, Wiley, New York 1994.

[34] N.B. Colthup, L.H. Daly, S.E. Wiberly, *Introduction to Infrared and Raman Spectroscopy*, 3rd ed., Academic Press, Boston 1990.

[35] R.K. Alan, G.A. Novruz, D. Jacek, P.M. Prabhu, C.H. Dennis, G. Alâattin, *Magnetic Resonance Chem.* **45**, 532 (2007).

[36] D. Shoba, S. Periandi, S. Boomadevi, S. Ramalingam, E. Fereyduni, *Spectrochim. Acta Part A* **118**, 438 (2014).

[37] M. Karabacak, Z. Cinar, M. Kurt, S. Sudha, N. Sundaraganesan, *Spectrochimica Acta Part A* **85**, 179 (2012).